



UNIVERSITY OF LEEDS

This is a repository copy of *Enhancing photovoltaic hosting capacity—A stochastic approach to optimal planning of static var compensator devices in distribution networks*.

White Rose Research Online URL for this paper:
<http://eprints.whiterose.ac.uk/150322/>

Version: Accepted Version

Article:

Xu, X, Li, J, Xu, Z et al. (2 more authors) (2019) Enhancing photovoltaic hosting capacity—A stochastic approach to optimal planning of static var compensator devices in distribution networks. *Applied Energy*, 238. pp. 952-962. ISSN 0306-2619

<https://doi.org/10.1016/j.apenergy.2019.01.135>

© 2019, Elsevier. This manuscript version is made available under the CC-BY-NC-ND 4.0 license <http://creativecommons.org/licenses/by-nc-nd/4.0/>.

Reuse

This article is distributed under the terms of the Creative Commons Attribution-NonCommercial-NoDerivs (CC BY-NC-ND) licence. This licence only allows you to download this work and share it with others as long as you credit the authors, but you can't change the article in any way or use it commercially. More information and the full terms of the licence here: <https://creativecommons.org/licenses/>

Takedown

If you consider content in White Rose Research Online to be in breach of UK law, please notify us by emailing eprints@whiterose.ac.uk including the URL of the record and the reason for the withdrawal request.



eprints@whiterose.ac.uk
<https://eprints.whiterose.ac.uk/>

1 Enhancing photovoltaic hosting capacity—A 2 stochastic approach to optimal planning of static var 3 compensator devices in distribution network

4 Xu Xu^a, Jiayong Li^a, Zhao Xu^{a,*}, Jian Zhao^{a,b}, Chun Sing Lai^{c,d}

5 ^a Department of Electrical Engineering, The Hong Kong Polytechnic University, Hong Kong

6 ^b College of Electrical Engineering, Shanghai University of Electric Power, Shang Hai, China

7 ^c School of Civil Engineering, Faculty of Engineering, University of Leeds, Leeds, LS2 9JT, U.K.

8 ^d Department of Electrical Engineering, School of Automation, Guangdong University of Technology, Guangzhou, 510006,
9 China

10 **Abstract**—To improve photovoltaic (PV) hosting capacity of distribution networks (DN), this paper proposes a novel
11 optimal static VAR compensator (SVC) planning model which is formulated as a two-stage stochastic programming
12 problem. Specifically, the first stage of our model determines the SVC planning decisions and the corresponding PV hosting
13 capacity. In the second stage, the feasibility of the first stage results is evaluated under different uncertainty scenarios of
14 load demand and PV output to ensure no constraint violations, especially no voltage violations. In addition, we
15 simultaneously consider the minimization of SVC planning cost and the maximization of PV hosting capacity by
16 formulating a multi-objective function. To improve the computational efficiency, a solution method based on Benders
17 decomposition is developed by decomposing the two-stage problem into a master problem and multiple subproblems.
18 Finally, the effectiveness of the proposed model and solution method is validated on modified IEEE 37-node and 123-node
19 distribution systems.

20
21 **Keywords**—Photovoltaic (PV) hosting capacity, distribution networks (DNs), static VAR compensator (SVC) planning
22 model, two-stage stochastic programming problem, uncertainty scenarios of load demand and PV output, Benders
23 decomposition

24

* Corresponding author. Tel.: +852 2766 6160.
E-mail address: eezhaoxu@polyu.edu.hk (Z. Xu).

25

26

Nomenclature	
Sets and Indices	
i / N	Index/set of distribution nodes.
m	Index of nodes with PV generation installation.
$N^{PV}(i)$	Set of child nodes of the node i with PV generation units.
t / T	Index/set of time periods.
s / S	Index/set of scenarios.
Variables	
P_{its} / Q_{its}	Active/Reactive power flow through the branch between node $i-1$ and node i in period t and scenario s (kW/kVAR).
V_{its}	Node voltage at node i in period t and scenario s .
a_i^{SVC}	Binary decision variable flagging SVC installation at node i or not.
Q_i^{SVC}	SVC installation capacity at node i (kVAR).
q_{its}^{SVC}	Reactive power support of SVC at node i in period t and scenario s .
E_m^{PV}	PV hosting capacity allocated to node m .
$\bar{s}_{its} / \underline{s}_{its}$	Slack variable for upper/lower bound of voltage magnitude at node i in period t and scenario s .
Parameters	
w^{PV}	Weighting factor of the PV hosting capacity.
w^{SVC}	Weighting factor of the SVC planning cost, including SVC investment cost and SVC operation cost.
C_F^{SVC}	Objective function coefficient associated to the fixed investment cost of SVC (\$).
C_V^{SVC}	Objective function coefficient associated to the varying operation cost of SVC (\$/h).
$C^{Penalty}$	Objective function coefficient associated to the penalty cost for voltage violation (\$/p.u.).
p_s	Probability of scenario s occurrence.
N_{inv}^{SVC}	Maximum allowed total SVC installation number.
ξ_{its}^{PV}	PV output factor (ratio of PV hosting capacity) in period t and scenario s , $\xi_{its}^{PV} \in [0,1]$
p_{mst}^{PV}	PV output of unit m in period t and scenario s (kW).

27

28 1. Introduction

29 The proliferation of renewable distributed generation (RDG), especially photovoltaic (PV) generation, is a promising strategy
30 to address the worldwide energy and environmental concerns. The widespread use of PV generation technologies has a lot of
31 benefits such as reducing energy cost and emission, deferring upgrade of transmission network, and relieving reliance on fossil
32 fuels [1, 2]. On the other hand, the overuse of PV generation may disrupt normal power system operating conditions, like overload
33 of distribution lines and voltage constraints, due to the lack of advanced control schemes [3, 4]. To maintain the reliable and secure
34 operation of power systems, a large amount of PV curtailment has been observed across the world [5], particularly in China [6].
35 Therefore, it is critically import to improve the PV hosting capacity of power systems, especially the distribution networks (DNs).

36 PV hosting capacity is defined as the maximum total PV capacity that a DN can accommodate without violating operational
37 constraints, especially node voltage constraints. Various factors could impact PV hosting capacity like PV type, DN characteristics,
38 and limiting criteria defined by the DN operators [7-9]. Consequently, it is challenging to assess the PV hosting capacity of a DN.
39 The simulation-based approach is mostly used to evaluate the PV hosting capacity [10-13]. For example, Monte Carlo simulation

40 based stochastic analysis is employed to estimate PV hosting capacity in [13]. There are also some works focusing on the
41 improvement of PV hosting capacity. Ref. [14] investigates the potential of battery energy storage systems to improve the PV
42 penetration level. Ref. [15] develops a reactive power control method using RDG units to enhance the integration of renewable
43 energy. Ref. [16] explores how the RDG hosting capacity can be improved by means of static and dynamic network reconfiguration.
44 Ref. [17] uses active-management strategies (AMSS) to improve the RDG hosting capacity. However, most works focus on
45 enhancing the PV hosting capacity based on the short-term operation strategies and overlook the impact of the long-term planning,
46 which results in a very limited enhancing capability. Therefore, we endeavor to improve the PV hosting capacity from the
47 perspective of long-term planning.

48 The installation of SVC in the DN is envisioned to be an effective means to enhance the PV hosting capacity, since SVC is
49 capable of voltage regulation by absorbing or releasing reactive power. Traditionally, capacitor bank (CB) is utilized to compensate
50 reactive power in DNs due to its relatively low installation cost and maintenance cost. However, CB can only release reactive
51 power with discontinuous adjustment. Besides, overuse of CB will lead to the reduced lifetime. By contrast, SVC is capable of
52 consuming and compensating reactive power continuously with fast reaction in response to the voltage variations. Thus, SVC can
53 be employed to alleviate the overvoltage violations caused by the high PV generation. Hence, the placement of SVC has a
54 considerable influence on the PV hosting capacity. However, classical SVC planning studies [18-21] overlook the potential of
55 SVC planning for PV hosting capacity enhancement. For example, the SVC planning problem in [18] only focuses on addressing
56 the challenge of increasing load demand by strengthening the voltage regulation capability. Instead of improving the voltage
57 regulation performance, our work mainly focuses on maximizing the PV hosting capacity of the DN with optimal planning of
58 SVC.

59 There are various uncertainties in the DN, e.g. uncertain load demand and renewable energy output. Robust optimization (RO)
60 [22] and stochastic programming [23] are two typical methods to tackle the uncertainties. Compared with the stochastic
61 programming solutions, the solutions of RO are often considered to be over-conservative since RO gives too much emphasis on
62 the worst-case scenario whose occurrence probability is relatively low. Generally, stochastic programming is adopted to model the
63 power system planning problem by minimizing the expected cost over the multiple representative uncertainty scenarios subject to
64 all practical constraints. Thus, stochastic programming is more robust than the deterministic optimization but less conservative
65 than RO. We hence adopt stochastic programming to formulate our planning problem.

66 In this paper, we propose a novel optimal SVC planning model based on stochastic programming aiming at maximizing the
67 PV hosting capacity of the DN. In particular, the model is formulated as a two-stage problem, where the first stage is to determine
68 the PV hosting capacity and the SVC planning decisions, and the second stage is to ensure that there is no operation constraints
69 violation for any considered uncertainty scenarios given the predetermined first stage results. In addition, we develop an efficient

70 solution method based on the Benders decomposition to solve this two-stage stochastic problem. The effectiveness of the proposed
71 model and the solution method is verified on the modified 33-node and 123-node distribution systems. The major contributions
72 are summarized in threefold as below,

73 1) This paper proposes an effective and efficient way to enhance PV hosting capacity, which plays an important role in
74 identifying the capability of a DN to accommodate PV generations. Considering that SVC is widely used in power system, this
75 work investigates the potential benefits of optimal SVC planning for improving PV hosting capacity by offsetting the voltage rise
76 problems caused by PV integrations.

77 2) PV hosting capacity is difficult to be evaluated. Empirically, it is assessed using Monte Carlo simulation based approaches
78 like [13]. However, simulation-based approaches are time-consuming for the large systems and hardly applicable in studying PV
79 hosting capacity enhancement. In contrast, we originally model the PV hosting capacity as a decision variable in the optimization
80 context. Specially, we propose a novel two-stage SVC planning problem based on the stochastic programming and incorporate the
81 PV hosting capacity into the objective function. Thus, we can achieve a tradeoff between PV hosting capacity maximization and
82 the SVC planning cost minimization.

83 3) This paper develops a Benders decomposition-based solution method to efficiently solve the proposed two-stage planning
84 problem. To the best of the author's knowledge, this is the first study to employ Benders decomposition algorithm to solve the
85 two-stage SVC planning problem for PV hosting capacity improvement by far.

86 The rest of this paper is organized as follows. Section 2 gives the mathematical formulation of the stochastic programming
87 based optimal SVC planning model. Section 3 describes the solution methodology based on Benders decomposition. Section 4
88 describes the case studies to evaluate the effectiveness of the proposed planning model and solution approach. This is then followed
89 by the detailed analyses and discussion of results. Finally, concluding remarks are included in Section 5.

90 **2. Problem Formulation**

91 2.1. Two-stage Stochastic Framework

92 Fig. 1 depicts the two-stage stochastic framework of the proposed SVC planning problem in this paper. Practically, the first
93 stage decision variables are determined before the actual realization of the uncertain load demand and PV output, including the
94 sitting and sizing of SVC as well as evaluating the PV hosting capacity. On the other hand, the second stage decision variables
95 represent the operation decisions and thus depend on the uncertain realization. Therefore, we model the SVC planning problem as
96 a two-stage stochastic programming problem, where the first-stage variables are named as here-and-now decisions and the second-
97 stage variables are called wait-and-see decisions.

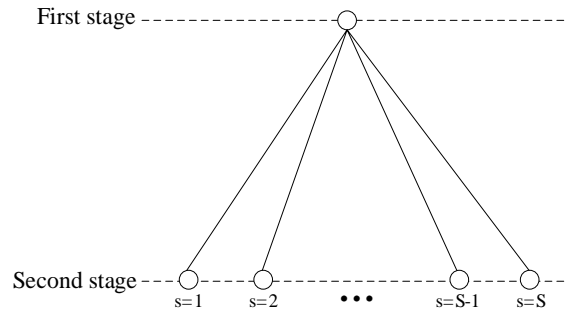


Fig. 1. Two-stage stochastic decision framework of the proposed SVC planning problem.

There are various uncertainties in the DN, e.g. uncertain load demand and renewable energy output. In this work, uncertainties of PV output and load demand are taken into consideration. These uncertainties are represented as the form of scenarios based on the historical data obtained from [24]. Specifically, we use about 3500 daily scenarios of PV output and load demand in Nordic countries over the past ten years, respectively. The original numerous scenarios need to be reduced to representative scenarios as the inputs of the stochastic planning process. The derived numerical scenarios should be reduced to a set of representatives to facilitate the stochastic programming. Here, a backward-reduction algorithm based on Kantorovich Distance (KD) [25] is employed due to its capability of generating the associated weights (probabilities) of the selected scenarios, which can distinguish the significance of the inputs of the subsequent stochastic planning stage. The procedure of this scenario reduction method is interpreted in [25].

2.2. DistFlow Model

Consider a distribution system with $n+1$ nodes indexed by $i = 0, 1, 2, \dots, n$ as shown in Fig. 2. The power flow equations can be described using DistFlow model [26, 27] as follows,

$$P_{i+1} = P_i - r_i \frac{P_i^2 + Q_i^2}{V_i^2} - p_i, \forall i \in N \quad (1a)$$

$$Q_{i+1} = Q_i - x_i \frac{P_i^2 + Q_i^2}{V_i^2} - q_i, \forall i \in N \quad (1b)$$

$$V_{i+1}^2 = V_i^2 - 2(r_{i+1} P_{i+1} + x_{i+1} Q_{i+1}) + (r_{i+1}^2 + x_{i+1}^2) \frac{P_{i+1}^2 + Q_{i+1}^2}{V_i^2}, \forall i \in N \quad (1c)$$

$$p_i = p_i^d - p_i^g, \forall i \in N \quad (1d)$$

$$q_i = q_i^d - q_i^g, \forall i \in N \quad (1e)$$

where equations (1a) and (1b) describe the active and reactive power balance at each node, respectively; Equation (1c) describes the voltage relationship between two adjacent nodes. In order to reduce the complexity, the linearized DistFlow equations are proposed by neglecting the high-order terms in (1a)-(1c). The effectiveness of this approximated model is verified in [26, 28].

115 Specifically, the linearized DistFlow equations are formulated as follows,

$$P_{i+1} = P_i - p_i, \forall i \in N \quad (2a)$$

$$Q_{i+1} = Q_i - q_i, \forall i \in N \quad (2b)$$

$$V_{i+1} = V_i - \frac{r_{i+1}P_{i+1} + x_{i+1}Q_{i+1}}{V_0}, \forall i \in N \quad (2c)$$

$$p_i = P_i^d - p_i^g, \forall i \in N \quad (2d)$$

$$q_i = Q_i^d - q_i^g, \forall i \in N \quad (2e)$$

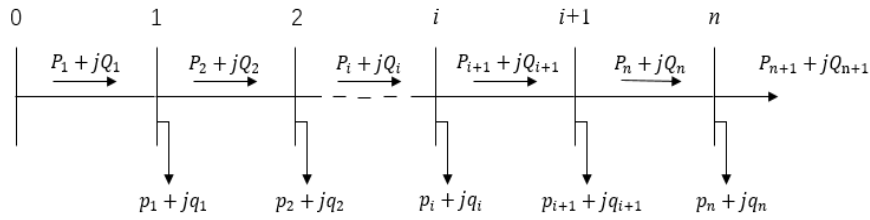


Fig. 2 Diagram of a radial distribution system.

116 2.3. PV Hosting Capacity Enhancement via Optimal SVC Planning

117 According to the linearized DistFlow equations (2a)-(2e), the voltage magnitude of node $i+1$ can be expressed as (2c). Thus,
 118 the voltage increment ΔV between can be formulated as $\Delta V = V_i - V_{i+1} = \frac{r_{i+1}P_{i+1} + x_{i+1}Q_{i+1}}{V_0}$. With the PV power penetration
 119 increase in the node i , the inverse active power flow P_{i+1} increases. Therefore, voltage increment ΔV increases, which may
 120 cause an overvoltage problem. However, SVC has the capability of offsetting the voltage rise via reactive power consumption.
 121 Specifically, SVC can absorb the reactive power to increase the reactive power flow Q_{i+1} , hence, the voltage increment ΔV
 122 decreases. Therefore, SVC is helpful in enhancing the PV hosting capacity.

123 2.4. Mathematical Formulation of SVC Planning Problem

124 Definition: PV hosting capacity is defined as the maximum total PV capacity that a DN can accommodate without violating
 125 operational constraints, especially node voltage constraints.

126 In this subsection, a novel stochastic planning of SVC is proposed to maximize PV hosting capacity of the DN. In particular,
 127 a two-stage stochastic programming model is formulated considering the uncertainties of load demand and PV output. The detailed
 128 planning model are described as follows:

129 2.4.1. Objective Function

130 We consider two objectives in our formulation. One is to maximize the PV hosting capacity as shown by Eq. (3a), and the

131 other is to minimize SVC planning cost consisting of investment cost and operation cost as shown by Eq. (3b).

$$\text{Max} \sum_m E_m^{\text{PV}} \quad (3a)$$

$$\text{Min} \sum_i \eta C_F^{\text{SVC}} a_i^{\text{SVC}} + \sum_s P_s \sum_t \sum_i C_V^{\text{SVC}} a_i^{\text{SVC}} |q_{\text{its}}^{\text{SVC}}| \quad (3b)$$

132 where $\eta = \frac{\text{ir}(1+\text{ir})^y}{365[(1+\text{ir})^y - 1]}$ represents the daily recovery factor, ir is the interest rate of SVC device, and y is the planning

133 horizon.

134 To deal with the above two objectives simultaneously, we construct a multi-objective function by formulating a weighted sum
135 function as below,

$$\text{Min}_{\psi_1, \psi_2} -w^{\text{PV}} \sum_m E_m^{\text{PV}} + w^{\text{SVC}} (\sum_i \eta C_F^{\text{SVC}} a_i^{\text{SVC}} + \sum_s P_s \sum_t \sum_i C_V^{\text{SVC}} a_i^{\text{SVC}} \tilde{q}_{\text{its}}^{\text{SVC}}) + C^{\text{Penalty}} \sum_s P_s \sum_t \sum_i (\bar{s}_{\text{its}} + \underline{s}_{\text{its}}) \quad (4)$$

136 where w^{PV} and w^{SVC} are weighting factors, and $w^{\text{PV}} + w^{\text{SVC}} = 1$. Different weighting factors will result in different tradeoff
137 between the PV hosting capacity (the first part) and SVC planning cost (the second part). In practice, these factors are adjustable

138 depending on the preference of distribution system planners; $\tilde{q}_{\text{its}}^{\text{SVC}} := |q_{\text{its}}^{\text{SVC}}|$; $\psi_1 = \{a_i^{\text{SVC}}, Q_i^{\text{SVC}}, E_m^{\text{PV}}\}$ and $\psi_2 = \{P_{\text{its}}, Q_{\text{its}}, V_{\text{its}}, q_{\text{its}}^{\text{SVC}}\}$

139 denote the collection of the first-stage variables and the collection of the second-stage variables, respectively. Note that the third
140 part of objective function (4) represents the penalty cost, which is imposed to avoid the occurrence of voltage violations.

141 Specifically, we introduce two non-negative slack variables \bar{s}_{its} and $\underline{s}_{\text{its}}$ to represent the overvoltage and undervoltage violations

142 in the second stage, respectively. If these two variables turn out to be positive, it means that E_m^{PV} obtained from the first stage

143 does not truly evaluate the PV hosting capacity. Hence, it will be revised until the slack variables \bar{s}_{its} and $\underline{s}_{\text{its}}$ both converge to

144 zero.

145 2.4.2. Constraints

146 The constraints are classified into first-stage constraints and second-stage constraints, where the first-stage constraints are
147 given as,

148 a) PV Hosting Capacity Limit

$$E_m^{\text{PV}} \geq 0, \forall m \in N^{\text{PV}}(i) \quad (5a)$$

149 where (5a) represents that the PV hosting capacity is non-negative.

150 b) SVC Installation Limit

$$0 \leq Q_i^{\text{SVC}} \leq \bar{Q}_i^{\text{SVC}}, \forall i \in N \quad (5b)$$

$$\sum_i a_i^{\text{SVC}} \leq N_{\text{inv}}^{\text{SVC}}, \forall i \in N \quad (5c)$$

151 where (5b) denotes the SVC installation capacity limit in which the upper bound represents the maximum available installation
 152 capacity of SVC in practical application. (5c) describes that the total SVC installation number cannot exceed a predefined number
 153 considering the limit of the total capital cost.

154 The second-stage constraints are given as,

155 a) Power Flow Constraints

$$P_{i+1ts} = P_{its} + p_{mns}^{\text{PV}} - p_{its}^{\text{d}}, \forall i \in N, \forall m \in N^{\text{PV}}(i), \forall t \in T, \forall s \in S \quad (6a)$$

$$\text{where } p_{mns}^{\text{PV}} = \xi_{ts}^{\text{PV}} E_m^{\text{PV}}$$

$$Q_{i+1ts} = Q_{its} + q_{lts}^{\text{SVC}} - q_{its}^{\text{d}}, \forall i \in N, \forall t \in T, \forall s \in S \quad (6b)$$

$$V_{i+1ts} = V_{its} - \frac{r_{i+1} P_{i+1ts} + x_{i+1} Q_{i+1ts}}{V_0}, \forall i \in N, \forall t \in T, \forall s \in S \quad (6c)$$

$$P_{i+1ts} \leq \bar{P}_i, \forall i \in N, \forall t \in T, \forall s \in S \quad (6d)$$

$$Q_{i+1ts} \leq \bar{Q}_i, \forall i \in N, \forall t \in T, \forall s \in S \quad (6e)$$

156 where (6a)-(6c) represent linearized DistFlow equations. Specially, (6a) and (6b) describes the active power flow and reactive
 157 power flow. To capture the uncertainty of PV output, we define the PV output factor $\xi_{ts}^{\text{PV}} \in [0,1]$ so that PV power p_{mns}^{PV} generated
 158 by distributed PV generator allocated to node m at time t in scenario s is $\xi_{ts}^{\text{PV}} E_m^{\text{PV}}$. (6c) describes the voltage transmit along the
 159 branch. (6d) and (6e) give the active and reactive power flow limits, respectively.

160 b) Voltage Magnitude Constraints

$$\underline{V}_i - \underline{s}_{ts} \leq V_{its} \leq \bar{V}_i + \bar{s}_{ts}, \forall i \in N, \forall t \in T, \forall s \in S \quad (6f)$$

$$\bar{s}_{ts} \geq 0, \underline{s}_{ts} \geq 0, \forall i \in N, \forall t \in T, \forall s \in S \quad (6g)$$

161 where (6f) shows the relaxed voltage constraints with two slack variables \bar{s}_{ts} and \underline{s}_{ts} , and (6g) shows that these slack variables
 162 are non-negative.

163 c) SVC Operation Constraints

$$-a_i^{\text{SVC}} Q_i^{\text{SVC}} \leq q_{lts}^{\text{SVC}} \leq a_i^{\text{SVC}} Q_i^{\text{SVC}}, \forall i \in N, \forall t \in T, \forall s \in S \quad (6h)$$

$$\tilde{q}_{lts}^{\text{SVC}} \geq q_{lts}^{\text{SVC}}, \forall i \in N, \forall t \in T, \forall s \in S \quad (6i)$$

$$\tilde{q}_{lts}^{\text{SVC}} \geq -q_{lts}^{\text{SVC}}, \forall i \in N, \forall t \in T, \forall s \in S \quad (6j)$$

164 where (6h) imposes limit on the reactive power support of SVC. (6i) and (6j) are used to convert the term $|q_{lts}^{\text{SVC}}|$ to $\tilde{q}_{lts}^{\text{SVC}}$. Note

165 that there is a bilinear term $a_i^{SVC} Q_i^{SVC}$ in constraint (6e), which renders the problem nonconvex. Hence, we introduce an auxiliary
 166 variable z_i^{SVC} to replace $a_i^{SVC} Q_i^{SVC}$ with four additional linear inequalities as shown by (7a)-(7b).

$$-a_i^{SVC} \bar{Q}_i^{SVC} + z_i^{SVC} \leq 0, \forall i \in N \quad (7a)$$

$$a_i^{SVC} \underline{Q}_i^{SVC} - z_i^{SVC} \leq 0, \forall i \in N \quad (7b)$$

$$-a_i^{SVC} \underline{Q}_i^{SVC} + z_i^{SVC} \leq Q_i^{SVC} - \underline{Q}_i^{SVC}, \forall i \in N \quad (7c)$$

$$a_i^{SVC} \bar{Q}_i^{SVC} - z_i^{SVC} \leq -Q_i^{SVC} + \bar{Q}_i^{SVC}, \forall i \in N \quad (7d)$$

167 By doing so, the nonlinearity is eliminated. Thus, (6e) is equivalently rewritten as (8).

$$-z_i^{SVC} \leq q_{its}^{SVC} \leq z_i^{SVC}, \forall i \in N, \forall t \in T, \forall s \in S \quad (8)$$

168 3. Solution to the optimization problem

169 In this section, we propose a solution method based on Benders decomposition to solve the proposed two-stage stochastic
 170 planning problem. Usually, the proposed stochastic planning problem is intractable because of numerous scenarios and time
 171 coupling objective. Thus, this problem cannot be directly solved by the commercial solvers, which is further demonstrated in the
 172 case studies. In this respect, we develop a solution method based on Benders decomposition to solve this planning problem.
 173 Generally, Benders decomposition is used to reduce the problem complexity by decomposing the original problem into a master
 174 problem and a subproblem. In addition, Benders cuts are generated and added to the master problem to build a link between the
 175 master problem and the subproblem. As aforementioned, our proposed problem is a two-stage problem and thus it is logical to
 176 apply Benders decomposition to solve it. The first stage of our problem corresponds to the master problem and the second stage
 177 problem corresponds to the subproblem. Moreover, we can decouple the coupled constraints and objective across the time horizon
 178 and uncertainty scenarios by further decomposing the second stage problem into multiple subproblems. Each subproblem is only
 179 associated with one time period and one scenario. Therefore, our proposed method can significantly improve the computational
 180 efficiency.

181 3.1. Subproblem

182 The subproblem for each scenario s and each time period t is given as,

$$Z_{ts}^{sub(v)} := \underset{\psi^{sp}}{\text{Min}} w^{SVC} \sum_i C_v^{SVC} a_i^{SVC(v)} \tilde{q}_{its}^{SVC(v)} + C^{Penalty} \sum_i (\bar{s}_{its}^{(v)} + \underline{s}_{its}^{(v)}) \quad (9a)$$

$$\text{s.t. (6a)-(6d), (6f)-(6i), (8)} \quad (9b)$$

$$E_m^{PV(v)} = E_m^{PV, fix} : \varphi_{nts}^{PV(v)}, \forall m \in N^{PV}(i) \quad (9c)$$

$$z_i^{\text{SVC}(v)} = z_i^{\text{SVC, fix}} : \varphi_{\text{its}}^{\text{SVC}(v)}, \forall i \in \mathbf{N} \quad (9d)$$

183 where v denotes the iteration index of Benders decomposition. $Z_{\text{ts}}^{\text{sub}(v)}$ denotes the optimal value of subproblem (9).

184 The decision variables of (9) is given by

$$185 \quad \psi^{\text{sp}} = \{Z_{\text{ts}}^{\text{sub}(v)}, E_m^{\text{PV}(v)}, z_i^{\text{SVC}(v)}, P_{\text{its}}^{(v)}, Q_{\text{its}}^{(v)}, Q_i^{\text{SVC}(v)}, a_i^{\text{SVC}(v)}, d_{\text{its}}^{\text{SVC}(v)}, \tilde{d}_{\text{its}}^{\text{SVC}(v)}, V_{\text{its}}^{(v)}, \bar{S}_{\text{its}}^{(v)}, \underline{S}_{\text{its}}^{(v)}, \varphi_{\text{mts}}^{\text{PV}(v)}, \varphi_{\text{its}}^{\text{SVC}(v)}\}$$

186 The objective function (9a) consists of SVC operation cost and penalty cost for voltage violations. (9b) summarizes the second-
187 stage constraints. $E_m^{\text{PV}(v)}$ and $z_i^{\text{SVC}(v)}$ are fixed in this subproblem as shown by (9c) and (9d), where $E_m^{\text{PV, fix}}$ and $z_i^{\text{SVC, fix}}$ are first
188 stage decision variables obtained from the master problem. After solving all the subproblems, we can obtain an upper bound $Z_{\text{upper}}^{(v)}$

189 to the optimal value of the original problem (4)-(8) as follows,

$$Z_{\text{upper}}^{(v)} = \sum_s p_s \sum_t Z_{\text{ts}}^{\text{sub}(v)} - w^{\text{PV}} \sum_m E_m^{\text{PV, fix}} + w^{\text{SVC}} \sum_i \eta C_F^{\text{SVC}} a_i^{\text{SVC, fix}} \quad (10)$$

190 Dual variables $\varphi_{\text{mts}}^{\text{PV}(v)}$ and $\varphi_{\text{its}}^{\text{SVC}(v)}$ of first-stage variables are used to calculate the sensitivities for generating Benders cuts.

191 These sensitivities can be obtained as follows,

$$\varphi_m^{\text{PV}(v)} = \sum_s p_s \sum_t \varphi_{\text{mts}}^{\text{PV}(v)}, \forall m \in \mathbf{N}^{\text{PV}}(i), \forall t \in \mathbf{T}, \forall s \in \mathbf{S} \quad (11a)$$

$$\varphi_i^{\text{SVC}(v)} = \sum_s p_s \sum_t \varphi_{\text{its}}^{\text{SVC}(v)}, \forall i \in \mathbf{N}, \forall t \in \mathbf{T}, \forall s \in \mathbf{S} \quad (11b)$$

192 3.2. Master Problem

193 The formulation of Benders master problem is given as,

$$Z_{\text{lower}}^{(v)} := \underset{\psi^{\text{mp}}}{\text{Min}} \lambda^{(v)} - w^{\text{PV}} \sum_m E_m^{\text{PV}(v)} + w^{\text{SVC}} \sum_i \eta C_F^{\text{SVC}} a_i^{\text{SVC}(v)} \quad (12a)$$

$$\text{s.t. (5a)-(5c), (7a)-(7b)} \quad (12b)$$

$$\lambda^{(v)} \geq \sum_s p_s \sum_t Z_{\text{ts}}^{\text{Sub}(k)} + \sum_m \varphi_m^{\text{PV}(k)} (E_m^{\text{PV}(v)} - E_m^{\text{PV}(k)}) + \sum_i \varphi_i^{\text{SVC}(k)} (z_i^{\text{SVC}(v)} - z_i^{\text{SVC}(k)}) \quad k = 1, 2, \dots, v-1 \quad (12c)$$

$$\lambda^{(v)} \geq \lambda^{\text{down}} \quad (12d)$$

$$\lambda^{(v)} - w^{\text{PV}} \sum_m E_m^{\text{PV}(v)} + w^{\text{SVC}} \sum_i \eta C_F^{\text{SVC}} a_i^{\text{SVC}(v)} \leq Z^{\text{opt}} \quad (12e)$$

194 The decision variables of (12) is given by

$$195 \quad \psi^{\text{mp}} = \{Z_{\text{lower}}^{(v)}, E_m^{\text{PV}(v)}, z_i^{\text{SVC}(v)}, Q_i^{\text{SVC}(v)}, a_i^{\text{SVC}(v)}, \lambda^{(v)}\}$$

196 The master problem (12) is a mixed-integer linear problem. $Z_{\text{lower}}^{(v)}$ is a lower bound of the original problem (4)-(8) since master
197 problem (12) relaxes the second-stage constraints. (12b) summarizes first-stage constraints. (12c) describes the Benders cut,
198 linking the master problem and the subproblem. (12d) introduces a lower bound λ^{down} for Benders cut $\lambda^{(v)}$ to accelerate the

199 convergence. (12e) guarantees that the objective value $Z_{\text{lower}}^{(v)}$ is lower or equal to the minimum upper bound Z^{opt} obtained from
 200 the subproblems.

201 3.3 Benders Decomposition Algorithm Procedure

202 The proposed bilevel Benders decomposition algorithm for solving the proposed two-stage stochastic SVC planning model is
 203 shown as Algorithm 1. The convergence is guaranteed until the upper bound meets the lower bound according to [29].

Algorithm 1 Benders Decomposition Algorithm

Step 1. Initialization: Set the iteration index $v=1$. Set the initial upper bound $Z_{\text{upper}}^{(v)} = \infty$ and lower bound $Z_{\text{lower}}^{(v)} = -\infty$. Set the convergence tolerance ε . Initialize the first-stage variables, $E_m^{\text{PV}(0)}$ and $z_1^{\text{SVC}(0)}$. Set $E_m^{\text{PV, fix}} = E_m^{\text{PV}(0)}$ and $z_1^{\text{SVC, fix}} = z_1^{\text{SVC}(0)}$.

Step 2. Iteration: Solve the subproblem (9) for each time period and each uncertainty scenario. Obtain the upper bound $Z_{\text{upper}}^{(v)}$ according to (10).

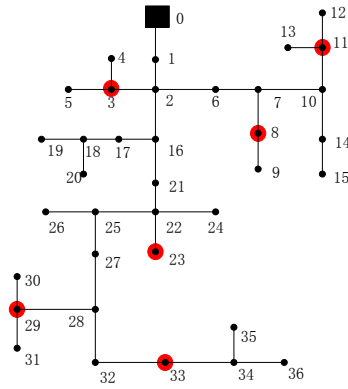
Step 3. Minimum upper bound update: If $Z_{\text{upper}}^{(v)} \leq Z^{\text{opt}}$, update the global solution $Z^{\text{opt}} = Z_{\text{upper}}^{(v)}$.

Step 4. Convergence check: If $|Z_{\text{upper}}^{(v)} - Z_{\text{lower}}^{(v)}| \leq \varepsilon$, then terminate with the optimal solution. Otherwise, calculate the sensitivities by equations (11a) and (11b) to build the next Benders cut. Then, set $v \leftarrow v+1$.

Step 5. Solve master problem: Solve the master problem (12), calculate $Z_{\text{lower}}^{(v)}$ and update the values of $E_m^{\text{PV, fix}}$ and $z_1^{\text{SVC, fix}}$. Then go back to the step 2 and continue.

204 4. Case Studies

205 4.1 Implementation on IEEE 37-node Distribution System



● Candidate location for PV installation

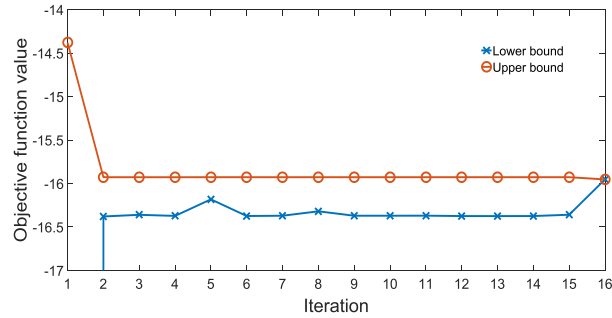
Fig. 3. Modified IEEE 37-node test distribution system.

206
207
208

209 Fig. 3 shows the IEEE 37-node test distribution system. We assume that there are six suitable locations for the PV installation,
 210 namely nodes 3, 8, 11, 23, 29 and 33. Details about the test system can be found in [30]. Per-unit value is used in case studies. The
 211 base values of power and voltage are set as 1 MVA and 12.66 kV, respectively. We consider a 10-year planning horizon. One
 212 hundred representative scenarios are generated to characterize the uncertainties. In this paper, as an example, one combination of
 213 weighting factor is selected to show the performance of our proposed model and algorithm, i.e. $w^{\text{PV}} = 0.5$ and $w^{\text{SVC}} = 0.5$.

214 4.1.1. Convergence Performance

215 Fig. 4 shows the convergence of the proposed Benders decomposition-based algorithm. Table 1 compares the computational
 216 efficiency of two approaches. One is to directly solve the original problem (4)-(8) using a commercial solver GUROBI [31] on
 217 the platform of CVX [32], denoted as CVX-GUROBI. The other is to solve the original problem (4)-(8) using our proposed
 218 Benders decomposition-based algorithm via the same platform and solver, demoted as CVX_BD-GUROBI. Table I demonstrates
 219 that the original problem (4)-(8) cannot be directly solved by the commercial solver GUROBI due to great computational
 220 complexity. However, our proposed algorithm is efficient in solving the same problem.



221
222 **Fig. 4.** Convergence of the proposed Benders decomposition based algorithm.

223
224 **Table 1**

225 Comparison on the computation time of solving the proposed SVC planning problem (under 100 scenarios).

CVX-GUROBI	CVX_BD-GUROBI	
[sec.]	[sec.]	[iterations]
NA	8211	16

226 *4.1.2. Optimal Results of PV Hosting Capacity and SVC Planning*

227 Table 2 lists PV hosting capacity for the selected sites. The total PV hosting capacity of the 37-node test distribution system is
 228 0.491 p.u. and the corresponding SVC planning decisions are shown in Table 3.

229 *4.1.3. Performance of SVC Planning Result on PV Hosting Capacity*

230 Fig. 5 depicts PV hosting capacity of two cases: 1) the base case without SVC installation; 2) the case with stochastic optimal
 231 SVC planning. It can be observed that the PV hosting capacity of case 2 is significantly higher than that of the case 1, which
 232 demonstrates the effectiveness of the stochastic optimal SVC planning in improving the PV hosting capacity. Fig. 6 shows the
 233 voltage profiles of node 13 at 1:00 pm under three cases: 1) base case (without installation of both PV and SVC), 2) case with PV
 234 installation as the result in Table 2 but without SVC installation, 3) case with PV installation as the result in Table II and SVC
 235 installation as the result in Table 3. It can be observed that voltage magnitudes of some nodes exceed the upper bound in case 2,
 236 but all overvoltage violations are alleviated after the optimal SVC planning as shown by the curve of case 3.

237 **Table 2**

238 Results of PV hosting capacity in 37-node test system.

Candidate location (Node)	PV size (p.u.)	Candidate location (Node)	PV size (p.u.)
3	0.121	23	0.109
8	0.082	29	0.036
11	0.062	33	0.081

239

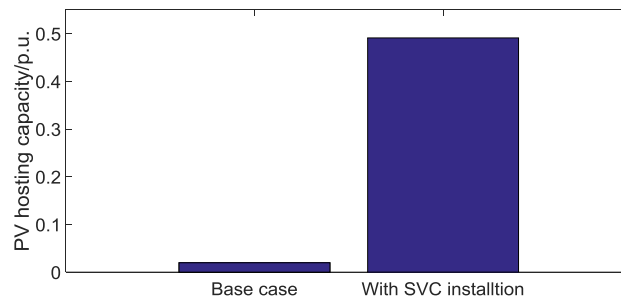
240

241 **Table 3**

242 Results of SVC planning in 37-node test system.

Location (Node)	SVC size (p.u.)	Location (Node)	SVC size (p.u.)
3	0.050	23	0.050
4	0.032	24	0.050
7	0.042	26	0.041
8	0.050	29	0.050
9	0.027	33	0.050
10	0.022	34	0.031
11	0.050	-	-

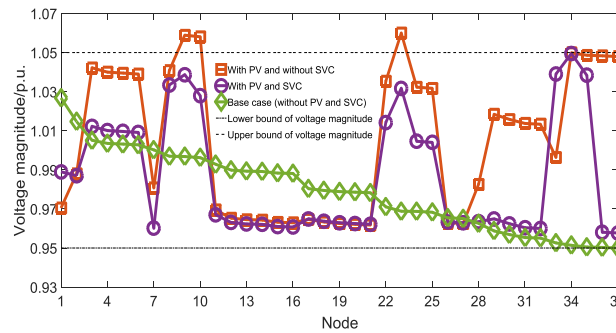
243



244

245

Fig. 5. Comparison on PV hosting capacity.



246

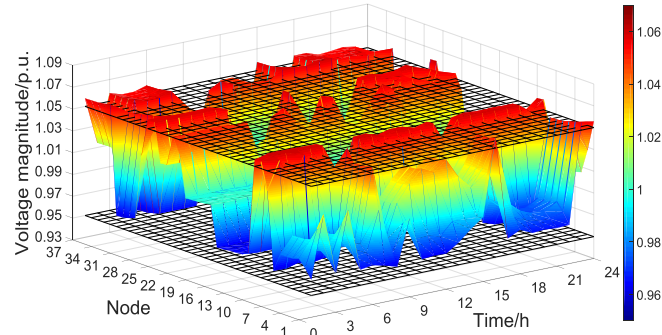
247

Fig. 6. Comparison on voltage profiles.

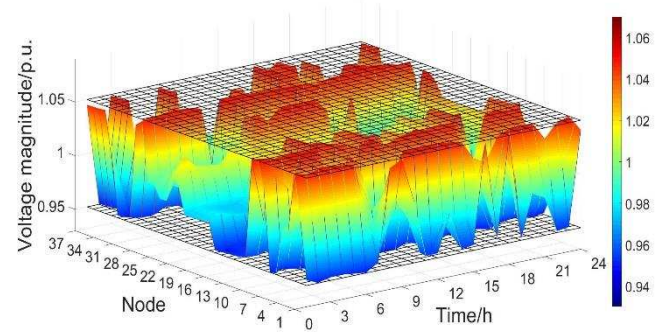
248 *4.1.4 Compared with Deterministic Scheme*

249 The deterministic SVC planning scheme is used as benchmark here. The formulation of the deterministic optimal SVC
 250 planning problem is similar to (4)-(8) but with only one scenario. The sites under the deterministic SVC planning scheme are node
 251 6, 7, 8, 9, 10, 11, 23, 24, 26, 29, 33 and 34. The corresponding sizes are 0.02, 0.035, 0.05, 0.05, 0.019, 0.05, 0.05, 0.043, 0.05,
 252 0.05, 0.05 and 0.043 p.u., respectively. We also obtain the PV hosing capacity under the deterministic scheme, i.e. 0.1, 0.07, 0.04,
 253 0.1, 0.03 and 0.06 p.u. for nodes 3, 8, 11, 23, 29, and 33, respectively. We define the critical scenario as the scenario with the
 254 highest PV power output factor ξ_{ts}^{PV} and lowest load demand level, and compare the performance of the stochastic result and the

255 deterministic result under this critical scenario. Fig. 7 (a) and (b) show the voltage profiles of the deterministic scheme and the
 256 stochastic scheme under the critical scenario, respectively. The overvoltage violations are observed in Fig. 7 (a), while there is no
 257 voltage violations in Fig. 7 (b). The reason is that stochastic scheme considers more scenarios and thus it is more comprehensive
 258 and robust in dealing with the uncertainties.



(a)



(b)

Fig. 7. Comparison result of (a) the deterministic scheme and (b) the stochastic scheme under the critical scenario.

261
 262
 263

264 4.1.5. Optimal Tradeoff Curve

265 Fig. 8 shows the optimal tradeoff curve between the PV hosting capacity and SVC planning cost. We can see that the PV
 266 hosting capacity increases linearly with the raise of the SVC planning cost until the cost reaches \$7,500. Then the increasing rate
 267 decreases gradually to zero, which means the PV hosting capacity becomes insensitive to the additional planning cost when the
 268 total cost exceeds \$1,7500.

269 4.1.6. Sensitivity Analysis

270 In order to investigate the impact of SVC installation capacity and number on the PV hosting capacity, two sensitivity

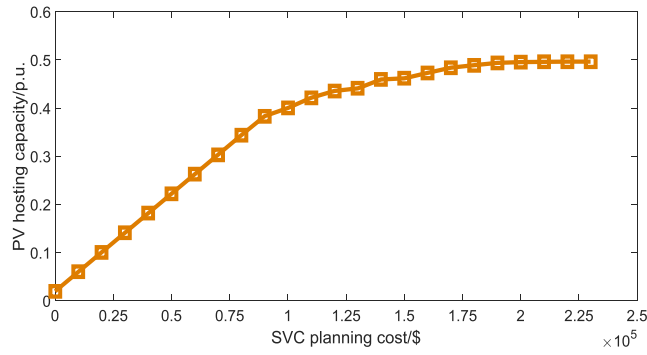
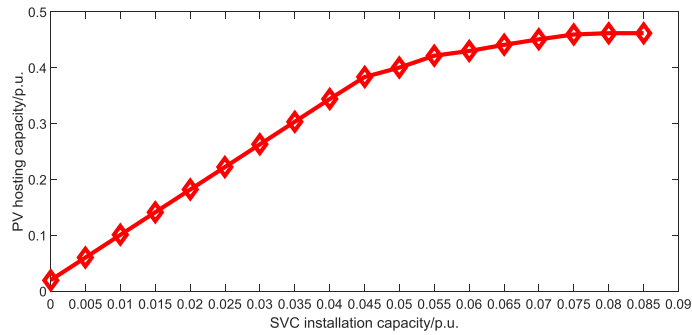
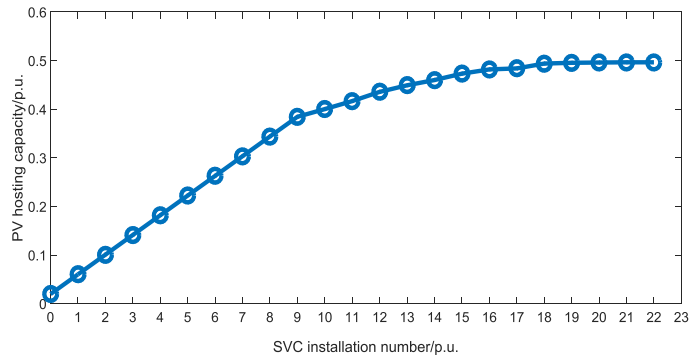


Fig. 8. Optimal tradeoff curve between the PV hosting capacity and SVC planning cost.

271 analyses are conducted. Fig. 9 (a) illustrates the impact of SVC installation capacity on the PV hosting capacity with the SVC
 272 installation number fixed at 10. Fig. 9 (b) illustrates the impact of SVC installation number on the PV hosting capacity with the
 273 installation capacity of each SVC being 0.05 per unit. It can be observed from Fig. 9 that the PV hosting capacity improves almost
 274 linearly with the increase of SVC installation capacity/number until the installation capacity reaches 0.045 p.u. and the installation
 275 number reaches 9. Then the PV hosing capacity becomes less sensitive and eventually insensitive to the increase of SVC
 276 installation capacity/number. This is because larger PV power penetration may lead to the DN line overload. Under such
 277 circumstance, DN line capacity expansion planning can be suggested if the PV hosting capacity is too small to be accepted by DN
 278 planners.



(a)

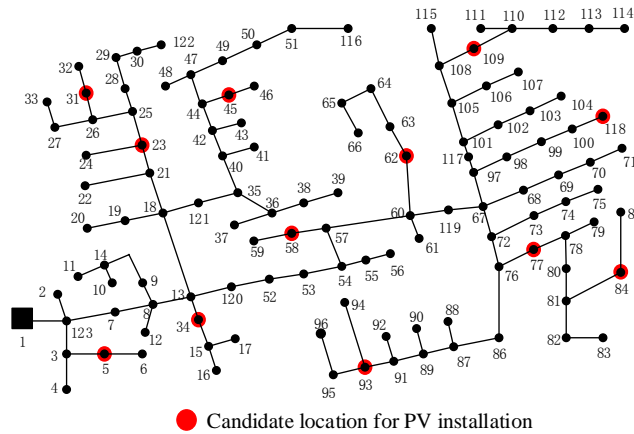


(b)

Fig. 9. Impact of (a) SVC installation capacity (with same installation number;10) and (b) SVC installation number (with same installation capacity: 0.05p.u.) on PV hosting capacity under the expected scenario.

287 4.2. Implementation on IEEE 123-node Distribution system

288 The proposed model is also tested on the modified IEEE 123-node distribution system as shown in Fig. 10. The detailed
 289 parameters can be found in [30]. In this case, base values of power and voltage, uncertainty scenarios and weighting factors are
 290 same as those in the 37-bus case. Twelve candidate locations are selected for the PV installation, i.e. nodes 5, 23, 31, 34, 45, 58,
 291 62, 77, 84, 93, 109 and 118. Results of PV hosting capacity and SVC planning are listed in Table IV and Table V, respectively.
 292 The total PV hosting capacity of the 123-node test distribution system is 2.459 per unit. The daily voltage magnitudes of the
 293 modified 123-node distribution system under the critical scenario are shown in Fig. 11. Similar to the 37-bus case, the voltage
 294 magnitudes are ensured within the allowable ranges.



295

296

Fig. 10. The modified IEEE 123-node test distribution system.

297

Table 4

298

Results of PV hosting capacity in 123-node system.

Candidate location (Node)	PV size (p.u.)	Candidate location (Node)	PV size (p.u.)
5	0.209	62	0.093
23	0.224	77	0.102
31	0.214	84	0.315
34	0.181	93	0.243
45	0.212	109	0.102
58	0.339	118	0.225

299

300

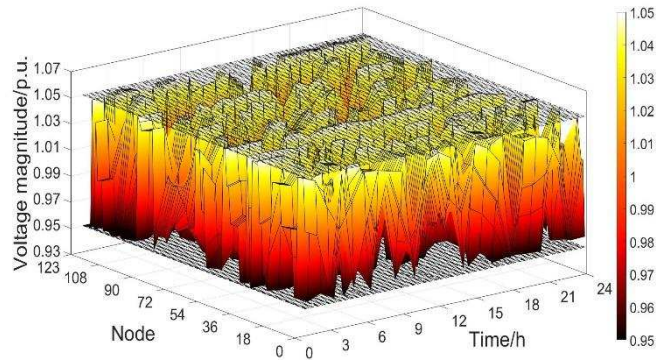
Table 5

301

Results of SVC planning in 123-node system.

Location (Node)	SVC size (p.u.)	Location (Node)	SVC size (p.u.)	Location (Node)	SVC size (p.u.)
5	0.050	37	0.009	84	0.050
6	0.034	45	0.050	85	0.036
22	0.015	47	0.040	93	0.050
23	0.050	57	0.043	94	0.048
25	0.003	58	0.050	109	0.050
30	0.043	59	0.050	117	0.008
31	0.050	62	0.050	118	0.050
33	0.044	77	0.050	119	0.028
34	0.050	83	0.050	-	-

302



303
304 **Fig. 11.** The daily voltage magnitudes of the modified 123-node distribution system under the critical scenario.

305 **6. Conclusion**

306 This paper presents a novel two-stage stochastic SVC planning model to enhance PV hosting capacity considering uncertainties
 307 of load demand and PV output. In the first stage, the SVC planning decisions and the corresponding PV hosting capacity are
 308 determined. In the second stage, the feasibility of the first stage decisions is evaluated under multiple uncertainty scenarios to
 309 ensure no voltage violations. To improve the computational efficiency, an efficient solution method based on Benders
 310 decomposition is developed to solve this two-stage problem. Numerical results on modified IEEE 37-node and 123-node
 311 distribution systems verify the effectiveness of the proposed model and solution method.

312 **Acknowledgment**

313 The authors gratefully acknowledge the support of Hong Kong RGC Theme based Research Scheme Grants No. T23-407/13N
 314 and T23-701/14N, Hong Kong Polytechnic University via grants G-YBY1 and G-YBLG.

315 **References**

- 316 [1] Walling R, Saint R, Dugan RC, Burke J, Kojovic LA. Summary of distributed resources impact on power delivery systems.
317 IEEE Transactions on power delivery. 2008;23:1636-44.
- 318 [2] Cervantes J, Choobineh F. Optimal sizing of a nonutility-scale solar power system and its battery storage. Applied Energy.
319 2018;216:105-15.
- 320 [3] Agüero JR. Improving the efficiency of power distribution systems through technical and non-technical losses reduction.
321 Transmission and Distribution Conference and Exposition (T&D), 2012 IEEE PES: IEEE; 2012. p. 1-8.
- 322 [4] Goop J, Odenberger M, Johnsson F. The effect of high levels of solar generation on congestion in the European electricity
323 transmission grid. Applied Energy. 2017;205:1128-40.
- 324 [5] Song J, Oh S-D, Yoo Y, Seo S-H, Paek I, Song Y, et al. System design and policy suggestion for reducing electricity curtailment
325 in renewable power systems for remote islands. Applied Energy. 2018;225:195-208.
- 326 [6] Sawin JL, Sverrisson F, Seyboth K, Adib R, Murdock HE, Lins C, et al. Renewables 2017 Global Status Report. 2013.
- 327 [7] Smith J, Rylander M. Stochastic analysis to determine feeder hosting capacity for distributed solar PV. Electric Power Research
328 Inst, Palo Alto, CA, Tech Rep. 2012;1026640.
- 329 [8] Ayres H, Freitas W, De Almeida M, Da Silva L. Method for determining the maximum allowable penetration level of distributed
330 generation without steady-state voltage violations. IET generation, transmission & distribution. 2010;4:495-508.
- 331 [9] Baran ME, Hooshyar H, Shen Z, Huang A. Accommodating high PV penetration on distribution feeders. IEEE Transactions
332 on smart grid. 2012;3:1039-46.
- 333 [10] Shayani RA, de Oliveira MAG. Photovoltaic generation penetration limits in radial distribution systems. IEEE Transactions
334 on Power Systems. 2011;26:1625-31.
- 335 [11] Dubey A, Santoso S, Maitra A. Understanding photovoltaic hosting capacity of distribution circuits. Power & Energy Society
336 General Meeting, 2015 IEEE: IEEE; 2015. p. 1-5.
- 337 [12] Dent CJ, Ochoa LF, Harrison GP. Network distributed generation capacity analysis using OPF with voltage step constraints.
338 IEEE Transactions on Power systems. 2010;25:296-304.
- 339 [13] Ding F, Mather B. On distributed PV hosting capacity estimation, sensitivity study, and improvement. IEEE Transactions on
340 Sustainable Energy. 2017;8:1010-20.
- 341 [14] Tant J, Geth F, Six D, Tant P, Driesen J. Multiobjective battery storage to improve PV integration in residential distribution
342 grids. IEEE Transactions on Sustainable Energy. 2013;4:182-91.
- 343 [15] Morren J, de Haan SW. Maximum penetration level of distributed generation without violating voltage limits. 2008.
- 344 [16] Capitanescu F, Ochoa LF, Margossian H, Hatziaargyriou ND. Assessing the potential of network reconfiguration to improve

- 345 distributed generation hosting capacity in active distribution systems. *IEEE Transactions on Power Systems*. 2015;30:346-56.
- 346 [17] Nursebo S, Chen P, Carlson O, Tjernberg LB. Optimizing wind power hosting capacity of distribution systems using cost
347 benefit analysis. *IEEE Transactions on Power Delivery*. 2014;29:1436-45.
- 348 [18] Mínguez R, Milano F, Zárate-Miñano R, Conejo AJ. Optimal network placement of SVC devices. *IEEE Transactions on*
349 *Power Systems*. 2007;22:1851-60.
- 350 [19] Mansour Y, Xu W, Alvarado F, Rinzin C. SVC placement using critical modes of voltage instability. *Power Industry Computer*
351 *Application Conference, 1993 Conference Proceedings: IEEE; 1993*. p. 131-7.
- 352 [20] Singh J, Singh S, Srivastava S. An approach for optimal placement of static VAR compensators based on reactive power spot
353 price. *IEEE Transactions on Power Systems*. 2007;22:2021-9.
- 354 [21] Savić A, Đurišić Ž. Optimal sizing and location of SVC devices for improvement of voltage profile in distribution network
355 with dispersed photovoltaic and wind power plants. *Applied Energy*. 2014;134:114-24.
- 356 [22] Ben-Tal A, El Ghaoui L, Nemirovski A. *Robust optimization: Princeton University Press; 2009*.
- 357 [23] Kall P, Wallace SW, Kall P. *Stochastic programming: Springer; 1994*.
- 358 [24] Haghighat H, Zeng B. Stochastic and chance-constrained conic distribution system expansion planning using bilinear benders
359 decomposition. *IEEE Transactions on Power Systems*. 2017.
- 360 [25] Growe-Kuska N, Heitsch H, Romisch W. Scenario reduction and scenario tree construction for power management problems.
361 *Power tech conference proceedings, 2003 IEEE Bologna: IEEE; 2003*. p. 7 pp. Vol. 3.
- 362 [26] Baran M, Wu FF. Optimal sizing of capacitors placed on a radial distribution system. *IEEE Transactions on Power Delivery*.
363 1989;4:735-43.
- 364 [27] Baran ME, Wu FF. Optimal capacitor placement on radial distribution systems. *IEEE Transactions on Power Delivery*.
365 1989;4:725-34.
- 366 [28] Baran ME, Wu FF. Network reconfiguration in distribution systems for loss reduction and load balancing. *IEEE Transactions*
367 *on Power Delivery*. 1989;4:1401-7.
- 368 [29] Sahinidis N, Grossmann IE. Convergence properties of generalized Benders decomposition. *Computers & Chemical*
369 *Engineering*. 1991;15:481-91.
- 370 [30] Singh D, Verma K. Multiobjective optimization for DG planning with load models. *IEEE Transactions on Power Systems*.
371 2009;24:427-36.
- 372 [31] Optimization G. Inc., "Gurobi optimizer reference manual," 2015. Google Scholar. 2014. (Provide website)
- 373 [32] Grant M, Boyd S, Ye Y. *CVX: Matlab software for disciplined convex programming. 2008*. (Provide website)